A Power-Efficient Formulation of Tandem-Hopped Radar & Communications

Brandon Ravenscroft [1], Patrick M. McCormick [1], Shannon D. Blunt [1], Erik Perrins [2], Justin G. Metcalf [3]
[1]Radar Systems Lab (RSL), University of Kansas, Lawrence, KS
[2]Communications & Signal Processing Lab (CSPL), University of Kansas, Lawrence, KS
[3]Sensors Directorate, Air Force Research Laboratory (AFRL), Wright-Patterson AFB, OH

***Abstract*—It was recently demonstrated that spectral notches in FM noise radar can be occupied by shaped OFDM subcarriers, thereby forming a composite far-field radar/communication emission that can be readily used for pulse compression matched filtering on receive. Here an optimization technique is presented that forms the composite waveform directly, such that the embedded OFDM subcarriers are part of a single constant amplitude multi-function signal that also possesses desirable autocorrelation properties. The impact on radar and communication performance is assessed by varying the number of embedded OFDM subcarriers, the size/structure of the symbol constellation, and their placement within the radar spectrum.**

Keywords*—*FM Noise Radar, Spectrum Sharing, Multi-function.

I. Introduction

Increasing spectral congestion [1] is driving research into a wide variety of strategies for spectrum sharing between radar and communications (e.g. [2]–[16]), which can coarsely be categorized as cohabitation or co-design, the latter including the multi-function systems. It was shown in [15] that one possible multi-function arrangement is to emulate the frequency-hopping spread spectrum (FH-SS) concept by inserting weighted OFDM subcarriers into a notch that is formed in the radar waveform spectrum. The weighting ensures the power spectrum of the composite radar + OFDM communication signal maintains a structure that provides an acceptable delay-Doppler ambiguity function, which is also aided by the tandem hopping of the notch/subcarriers around the radar spectrum.

This approach, denoted as tandem-hopped radar and communications (THoRaCs), relies on a notched instantiation of FM noise radar [17]–[20] that has been demonstrated experimentally. However, the OFDM component of THoRaCs does have the well-known drawback of potentially high peak-to-average power ratio (PAPR) [21]. Since the radar emission would likely need to be emitted at high power, and since OFDM has been shown to have limited utility for radar due to the associated power amplifier effects [22], the practical implementation of THoRaCs therefore necessitates separate transmitters for the radar and communication signals.

To address this limitation, here we investigate a variation of THoRaCs in which the composite radar + OFDM waveform is directly designed in the form of a single dual-purpose emission. This new emission structure, denoted as power-efficient THoRaCs (PE-THoRaCs), is optimized to provide undistorted communication subcarriers within a constant amplitude waveform possessing an acceptable delay-Doppler ambiguity function and is inherently suitable for high power transmission.

II. Waveform Optimization

Consider the design of a pulsed FM radar waveform of duration T and 3-dB bandwidth B that is required to possess low autocorrelation sidelobes while also containing N embedded OFDM subcarriers modulated with arbitrary quadrature amplitude modulation (QAM) communication symbols. Being FM, this waveform is naturally amenable to the rigors of a high-power radar transmitter. While it may seem counterintuitive for an OFDM signal to be subsumed within an FM waveform, it is the particular alternating projections optimization procedure in [13]- [14] that facilitates this realization by exploiting the available degrees of freedom within the radar time-bandwidth product BT. Further, it should be noted that this effect is <u>not</u> accomplished using the constant-envelope OFDM scheme [23]- [24], which requires more complicated symbol decoding on receive. Another constant-envelope OFDM-type signaling scheme is found in [25] but is applicable only for a multi-user uplink. Given knowledge of the subcarrier spectral locations within the radar band, the PE-THoRaCs emission only requires standard OFDM receive processing.

A total of M unique pulsed waveforms are constructed to form a radar coherent processing interval (CPI) yielding an overall time-bandwidth product of MBT. Each pulse is designed to approximate the desired power spectrum $|G(f)|^2$, which is chosen to be Gaussian here due to the associated Gaussian autocorrelation theoretically possessing no range sidelobes. The coherent combination of the echoes from these M pulses in the radar receiver (i.e. Doppler processing) provides further range sidelobe suppression due to their incoherence [17]- [18].

Given the particular OFDM subcarriers and symbols to be embedded, each pulsed waveform is independently optimized using a two-stage procedure. The first stage involves the cyclic repetition of three projections, each corresponding to a waveform property, namely: 1) matching the desired spectral shape $|G(f)|^2$, 2) matching to the structure of the QAM-modulated OFDM subcarriers, and 3) possessing a constant amplitude pulse shape of duration T. By repeated projection onto each of these sets, the solution descends onto a pulsed waveform that has attributes of all three desired properties, though it may not completely satisfy all the properties if the sets do not intersect (which is found to always be the case).

The second optimization stage ignores the desired spectral shaping and focuses only on the embedding of the communication signal into a constant amplitude pulse of length T. The rationale for this relaxation is that the first stage of cyclic projections produces a signal that sufficiently approximates the desired spectral shape (which is less stringent a requirement due to the coherent receive processing over the radar CPI). As such, the second stage emphasizes the stricter requirements of realizing undistorted communications and enforcing a finite pulse shape that is amenable to the high-power radar transmitter. These two projections are likewise repeated in a cyclic manner. The following details the specific operations in each stage.

A. PE-THoRaCs: Stage One

The mth pulse, defined over $-T/2 \leq t \leq +T/2$, is initialized with a random FM waveform denoted as $s_{0,m}(t)$ via a random instantiation of polyphase-coded FM (PCFM) [26]. This random FM waveform then undergoes three projections repeated cyclically, for k the cycle index. For the mth pulse, likewise let $r_m(t)$ for $-T/2 \leq t \leq +T/2$ be the communication signal, which is defined for the N subcarriers as

$$r_m(t) = \sum_{n=0}^{N-1} a_{m,n} |c_{m,n}| \exp[j(2\pi f_{m,n} t + \angle c_{m,n})], \quad (1)$$

where $f_{m,n}$ is the frequency of the nth subcarrier, $c_{m,n}$ is the QAM symbol encoded onto the nth subcarrier, $\angle(\bullet)$ is the phase of the argument, and $a_{m,n}$ is amplitude scaling that shapes the spectrum for the nth subcarrier.

The first projection imposes the spectral shaping

$$b_{k,m}(t) = \mathcal{F}^{-1}\left\{|G(f)| \exp\left(j\angle \mathcal{F}\left\{s_{k,m}(t)\right\}\right)\right\}, \quad (2)$$

where $\mathcal{F}$ and $\mathcal{F}^{-1}$ represent the Fourier and inverse Fourier transforms, respectively. Here $s_{k,m}(t)$ is being projected onto the set of waveforms having the power spectrum $|G(f)|^2$.

The second projection concurrently enforces a notch in the radar spectrum and inserts the communication signal via

$$\tilde{b}_{k,m}(t) = P_{\perp\, r_m}\left\{b_{k,m}(t)\right\} + r_m(t). \quad (3)$$

The operator $P_{\perp\, r_m}\{\bullet\}$projects the argument onto the orthogonal complement of the subcarrier frequencies in $r_m(t)$.

At this point it is unlikely that $\tilde{b}_{k,m}(t)$ is constant amplitude or strictly limited to a pulsewidth of T. Thus, the third projection satisfies these two constraints via the application of

$$s_{k+1,m}(t) = \begin{cases} \exp\left(j\angle\, \tilde{b}_{k,m}(t)\right) & |t| \leq T/2 \\ 0 & |t| > T/2 \end{cases}. \quad (4)$$

This sequence of projections is repeated K times to produce the constant amplitude waveform $s_{K,m}(t)$.

B. PE-THoRaCs: Stage Two

The second optimization stage uses cycle index ℓ and is initialized as $\tilde{s}_{\ell=0,m}(t) = s_{K,m}(t)$, followed by L iterations of

$$d_{\ell,m}(t) = P_{\perp\, r_m}\left\{\tilde{s}_{\ell,m}(t)\right\} + r_m(t) \quad (5)$$

and

$$\tilde{s}_{\ell+1,m}(t) = \begin{cases} \exp\left(j\angle\, d_{\ell,m}(t)\right) & |t| \leq T/2 \\ 0 & |t| > T/2 \end{cases}. \quad (6)$$

It has been found that, as long as the number of subcarriers is not too large a fraction of the waveform BT, the sets of signals resulting from (5) and (6) nearly always intersect. Thus $\tilde{s}_{L,m}(t)$ converges to a constant amplitude waveform of duration T that contains an OFDM communication signal and a spectrum shape that only marginally deviates from that realized in the first stage.

Note that the communication symbols in $r_m(t)$ can be drawn from arbitrary constellations, even those that possess amplitude modulation (e.g. higher order QAM). The two-stage optimization process can still realize a constant amplitude waveform by exploiting degrees of freedom contained in the waveform BT that are not associated with a subcarrier and corresponding symbol. It is for this reason that the number of embedded subcarriers cannot exceed too large a portion of the waveform time-bandwidth product, or else the optimization process cannot find a solution that satisfies both (5) and (6). Such an instance still produces a viable radar waveform, though an increase in the number of distortion-induced symbol errors will occur depending on how much the final application of (6) causes the waveform to deviate from satisfying (5).

III. Embedded OFDM Communication Parameters

In formulating the communication signal $r_m(t)$ we consider three design parameters that can be varied. These parameters are 1) the symbol constellation, 2) the number of OFDM subcarriers N relative to waveform BT, and 3) the placement strategy of these subcarriers within the radar spectrum. Here each subcarrier conveys a data-rate of only 1 symbol/pulse, higher values of which being another design parameter that could be examined.

While there are myriad different possible symbol constellations, three that are commonly used in conjunction with OFDM are 4-QAM, 16-QAM, and 64-QAM. The 4-QAM arrangement is the simplest as it is just a $\pi/4$ phase rotation of quadrature phase-shift keying (QPSK) and thus possesses only one symbol energy level since all the symbols reside on a single phase circle. In contrast, the 16-QAM constellation possess 4 possible amplitude values for each of the in-phase and quadrature-phase components as depicted in Fig. 1, which collectively correspond to 3 different energy levels. Likewise, the 64-QAM constellation (not shown) involves 8 possible in-phase and quadrature-phase amplitude values, resulting in 9 different symbol energy levels. Note that the presence of multiple subcarriers, along with M unique pulsed waveforms, allows these differing energy levels to partially average out to achieve the desired radar spectrum $|G(f)|^2$. This desired attribute is further ensured by the use of frequency hopping.

Three different strategies for the placement of OFDM subcarriers in the radar waveform are examined. For all three strategies, the N subcarriers are confined to reside in the 3-dB bandwidth B of the waveform. In the first strategy ("Contiguous Fixed"), the subcarriers occupy N contiguous frequencies at a fixed spectral location for all M pulses. For the second strategy ("Contiguous Hopped"), the subcarriers again occupy N contiguous frequencies, but their spectral location is randomly changed within B for each pulse. The third strategy ("Non-contiguous Hopped") then allows the N subcarriers to occupy non-contiguous spectral locations that are randomized for each pulse. Clearly the communication receiver would be required to know the hopping patterns for the 2nd and 3rd strategies.

Finally, the number of subcarriers N is defined as a percentage of the waveform time-bandwidth product BT. Here we consider 25%, 50%, and 75%. Higher $\%BT$ is expected to cause more distortion-induced symbol errors, particularly for denser constellations, since it becomes more difficult to meet

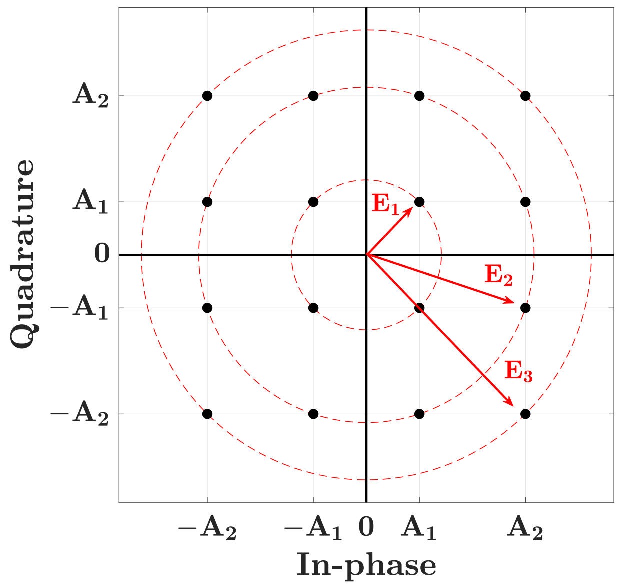

Fig. 1: 16-QAM constellation with energy levels shown

all the waveform design requirements.

In the context of typical radar operating specifications and these communication design values, one can determine the total data rates that are achievable. For example, consider $BT = 200$, a pulse repetition frequency (PRF) of 10 kHz, and assume a per subcarrier data rate of 1 symbol/pulse. Thus 25% BT occupancy (N = 200 x 0.25 = 50) and 4-QAM (2 bits/symbol) would yield a total data rate of 1 Mb/s, while 75% BT (N = 200 x 0.75 = 150) and 64-QAM (6 bits/symbol) would provide 9 Mb/s. However, it will be shown that the latter parameterization is impractical because there are insufficient design degrees of freedom to meet all the requirements.

IV. Simulation Results

Performance is assessed for the individual radar and communication attributes of the proposed dual-function waveform. For efficacy as a useful radar waveform we evaluate the mean autocorrelation over the CPI of M pulses, the RMS spectral content over the CPI, and the point-spread function obtained by performing pulse compression and Doppler processing for a hypothetical point scatterer. The communication performance is evaluated using the symbol error rate (SER).

For this assessment, there are $M = 10^4$ unique pulsed waveforms, each with $BT = 200$, thus yielding an overall time-bandwidth product of 2 x 10^6 for the entire CPI, which provides a coherent integration gain of 63 dB. Along with the symbol constellations of 4-QAM, 16-QAM, and 64-QAM, the %BT values of 25%, 50%, and 75% correspond to N = 50, 100, and 150 subcarriers per pulse, respectively. The "Contiguous Fixed" version of each of these configurations occupies a spectral interval in the center of the radar passband. The "Contiguous Hopped" and "Non-contiguous Hopped" subcarriers are randomly assigned within B on an independent basis for each pulse.

A. RMS Spectra and Autocorrelation Responses

Figure 2 shows the RMS spectra averaged over all $M = 10^4$ pulses for a 4-QAM constellation with subcarriers placed in a "Contiguous Fixed" manner. The desired Gaussian spectral template is shown as well. It is readily apparent that a better match to the desired spectral shape is achieved when the number of embedded OFDM subcarriers is a smaller percentage of the waveform BT. The spectra passbands are shown in the detail inset, where we find the most significant deviation occurring due to increased $\%BT$.

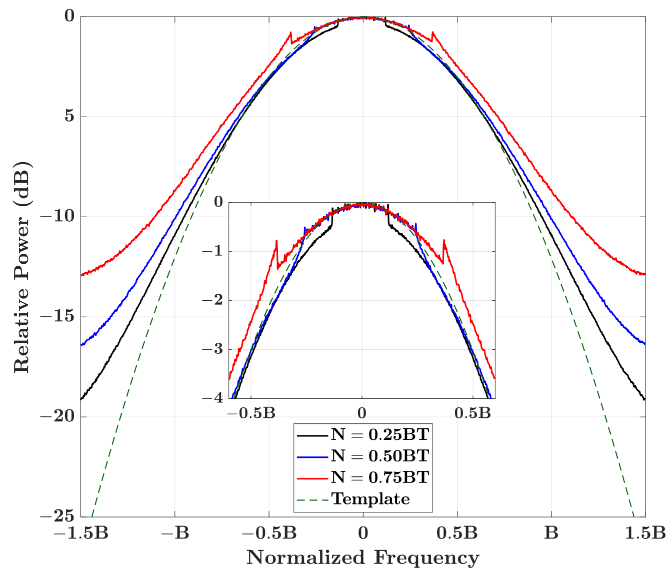

Fig. 2: RMS spectra for 4-QAM and Contiguous Fixed subcarriers

Figure 3 shows the mean autocorrelation across all $M = 10^4$ pulses (i.e. Doppler processing at zero Doppler) corresponding to the RMS spectra in Fig. 2. A detail inset is provided to highlight the range sidelobe response near the mainlobe. Marginally lower sidelobes are obtained for the waveforms with a smaller number of subcarriers, which is due to the better approximation to a Gaussian spectrum. It has been observed that the RMS spectra and mean autocorrelation responses for "Contiguous Fixed" subcarrier placement do not appreciably differ for the 16-QAM and 64-QAM constellations.

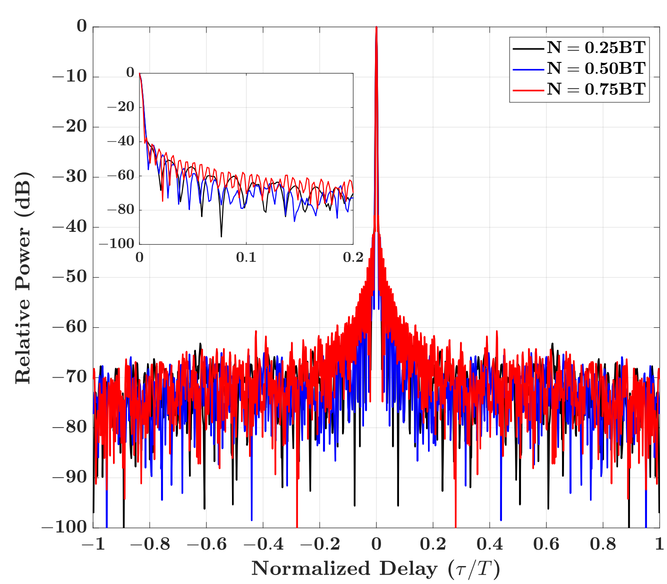

Fig. 3: Mean autocorrelation for 4-QAM and Contiguous Fixed subcarriers

Figure 4 shows the RMS spectra for a 64-QAM constellation with “Contiguous Hopped” subcarriers. It is again observed that a smaller number of subcarriers yields a spectrum that more closely matches the Gaussian template. The detail inset for the spectra passbands shows a much smoother response than that observed for “Contiguous Fixed” subcarriers, though the 75% BT still realizes some broadening. Figure 5 likewise shows the mean autocorrelation for “Contiguous Hopped” subcarriers, where the similar trend of modestly lower sidelobes for decreased $\%BT$ is found.

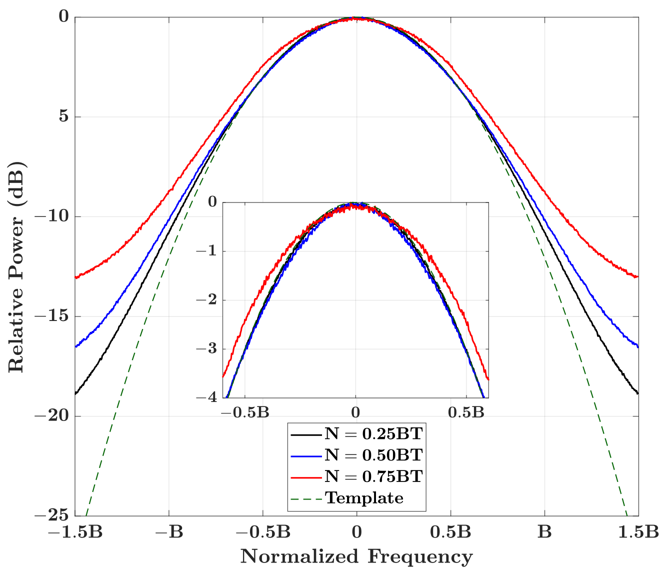

Fig. 4: RMS spectra for 64-QAM and Contiguous Hopped subcarriers

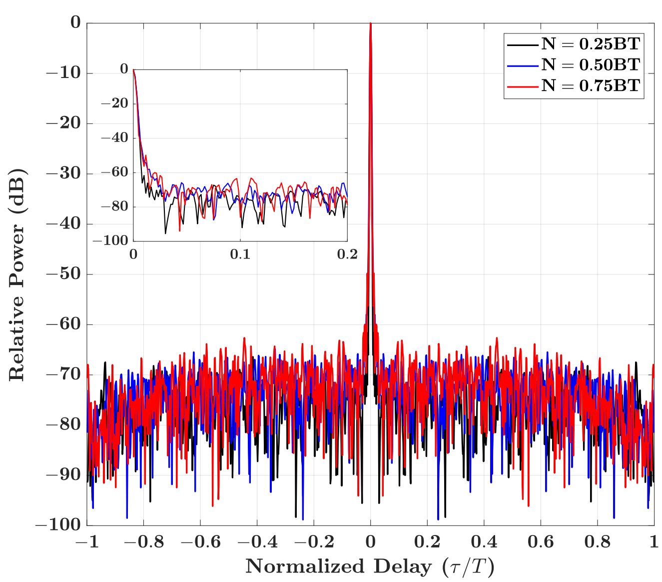

Fig. 5: Mean autocorrelation for 64-QAM and Contiguous Hopped subcarriers

Finally, Fig. 6 shows the RMS spectra for a 64-QAM constellation with “Non-contiguous Hopped” subcarriers. It is again observed that using a smaller number of subcarriers yields a mean spectrum that more closely approximates the Gaussian template. The detail inset also shows a better passband fit to the template for all values of N than was achieved for either of the contiguous subcarrier cases.

Likewise, Fig. 7 depicts the mean autocorrelation for “Non-contiguous Hopped” subcarriers. Once again, a more favorable autocorrelation response is obtained for the smaller number of subcarriers due to a better approximation of the spectral template. Here the 4-QAM and 16-QAM results were not included because their spectra was not appreciably different and the 64-QAM autocorrelation sidelobes were, by a small margin, the worst of the three.

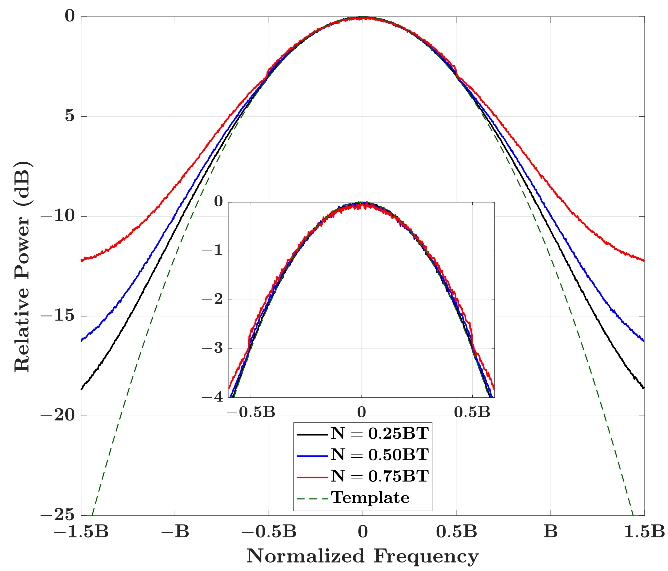

Fig. 6: RMS spectra for 64-QAM and Non-contiguous Hopped subcarriers

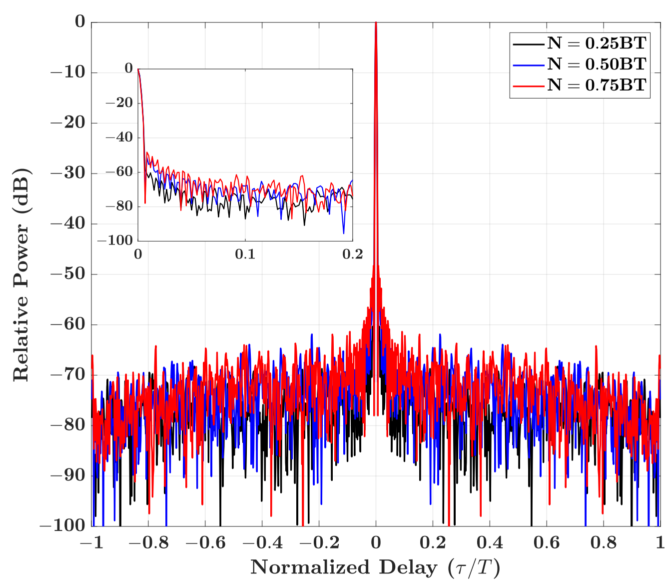

Fig. 7: Mean autocorrelation for 64-QAM and Non-contiguous Hopped subcarriers

The take away from these three sets of results is that, aside from some relatively small differences in passband spectra and very modest changes in what are still quite low sidelobe levels, the performance of these waveforms from a radar perspective is essentially unaffected by the amount of communication content incorporated into the radar waveform or how the subcarriers are allocated within the radar spectrum. Further, if we take the worst performing of the lot, namely N=0.75BT "Contiguous Fixed" subcarriers with a 4-QAM constellation, the resulting point-spread function (pulse compressed and Doppler processed across the M pulses) in Fig. 8 shows a response with very low delay/Doppler sidelobes outside the usual zero-delay $sin(x)/x$ Doppler sidelobes, which can be easily reduced by Doppler windowing across the pulses.

The reason why the inclusion of OFDM subcarriers has so little impact on radar performance for these waveforms is that they are already a form of FM noise radar [17]- [18]. The communication component may vary the structure of the waveforms but as long as they generally retain a Gaussian-like power spectrum and are sufficiently unique from pulse-to-pulse, the autocorrelation and point-spread performance will remain satisfactory.

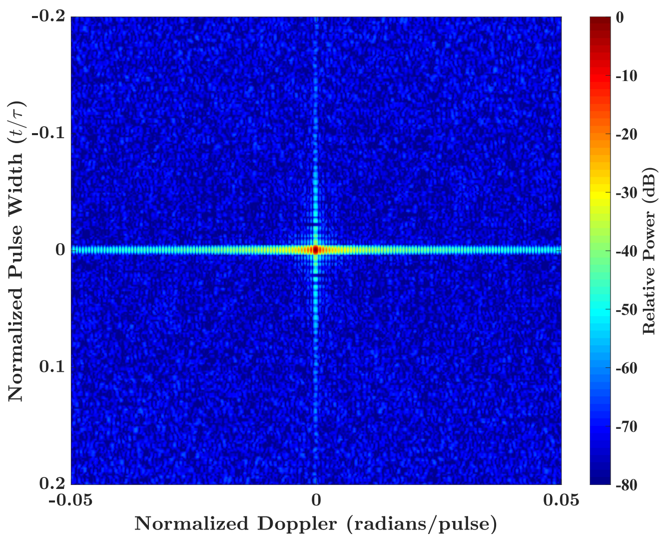

Fig. 8: Delay-Doppler point-spread function for 4-QAM and Contiguous Fixed subcarriers with $N = 0.75BT$

B. Symbol Error Rate Analysis

To characterize the communication performance of these dual-function waveforms the SER is evaluated. Each possible combination of the three subcarrier placement strategies, the three symbol constellations, and the three $\%BT$ values are considered. Additive complex Gaussian white noise (AWGN) is generated and added to each waveform and varied as a function of average SNR from 10 dB to +30 dB.

Figure 9 shows SER waterfall plots for all three symbol constellations and all three subcarrier placement strategies when $N = 0.25BT$. As expected, the higher constellation density requires a higher SNR to achieve the same SER. While some of these SNR values are quite high, bear in mind that these signals are being emitted from a radar transmitter, which could very well involve Megawatts of peak power. It is also observed that the "Contiguous Fixed" subcarrier arrangement is consistently better in terms of SER, which is not surprising here since those subcarriers were placed around the center of the passband where the spectral power content is highest.

It is also important to note that a single bit error produces a symbol error, and thus higher order constellations are disproportionately penalized when assessing SER. Converting to bit error rate (BER) can be more meaningful from a communication perspective, but the formulation of SER in terms of SNR is more convenient when considering the interaction with radar, which is likewise posed in terms of SNR.

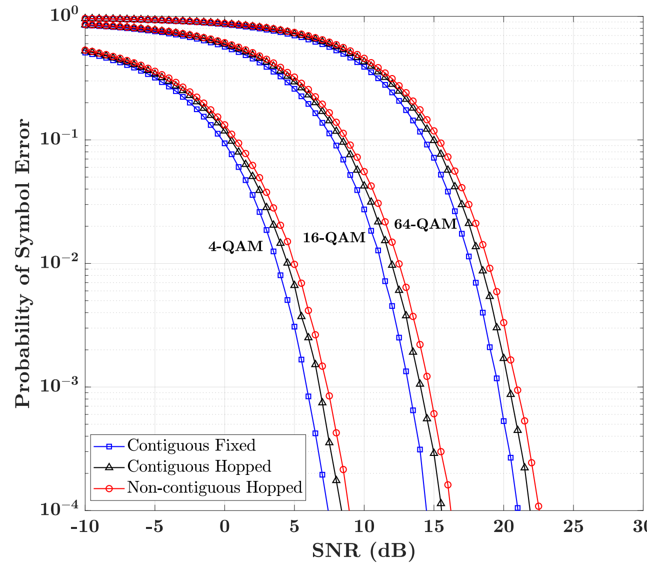

Fig. 9: SER for $N = 0.25BT$ subcarriers

Figures 10 and 11 generally show similar SER trends for $N = 0.50BT$ and $N = 0.75BT$, respectively. However, the "Contiguous Fixed" and "Contiguous Hopped" cases for 64-QAM when $N = 0.50BT$ and for both 64-QAM and 16-QAM when $N = 0.75BT$ reveal the emergence of a distortion-induced SER floor. These effects are occurring because the optimization process is not able to meet all of the requirements being made upon it and, while good FM noise radar waveforms of constant amplitude and pulsewidth T are still ensured, the communication component is distorted. These results highlight the fact that the parameterization of this radar/communication trade-space must be carefully considered when designing such waveforms.

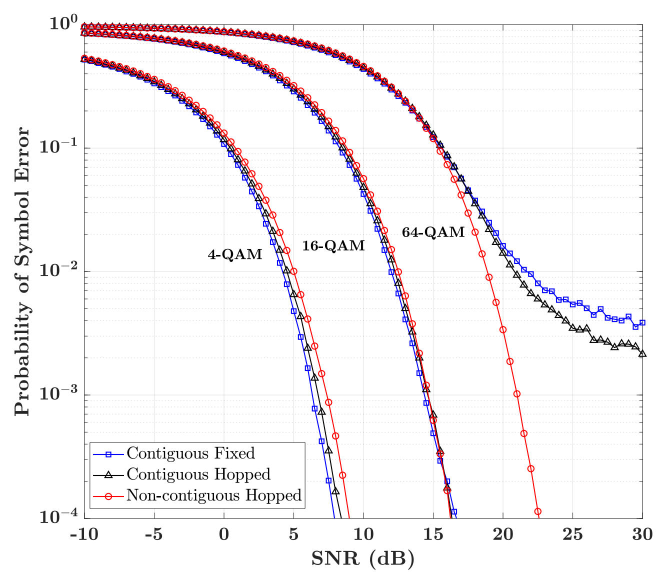

Fig. 10: SER for $N = 0.50BT$ subcarriers

V. Conclusion

A new dual-function radar/communication waveform has been developed that, by virtue of a two-stage optimization

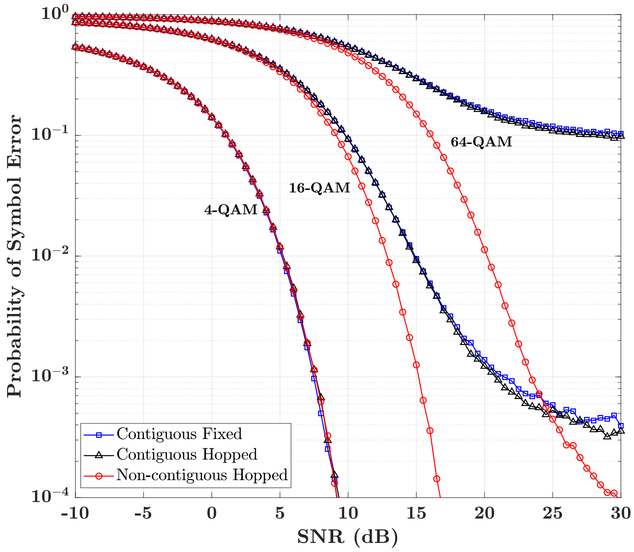

Fig. 11: SER for $N = 0.75BT$ subcarriers

process, can produce constant-amplitude pulsed radar waveforms with favorable delay/Doppler ambiguity properties that additionally contain OFDM subcarriers capable of achieving data rates on the order of Mb/s. Thus the typical high transmit power requirement for radar can be achieved while facilitating this dual-function operation that may have application to a variety of tactical scenarios. Simulation results have demonstrated a trade-off between the number of embedded subcarriers, the symbol constellation order, spectral containment, and SER performance. This manner of OFDM implementation may also prove useful to achieve communication-only waveforms with PAPR = 0 dB [27].

Acknowledgment

This work was supported by a subcontract with Matrix Research, Inc. for research sponsored by the Air Force Research Laboratory under Prime Contract #FA8650-14-D-1722.

References

[1] H. Griffiths, L. Cohen, S. Watts, E. Mokole, C. Baker, M. Wicks, and S. Blunt, "Radar spectrum engineering and management: Technical and regulatory issues," *Proceedings of the IEEE*, vol. 103, no. 1, pp. 85–102, Jan 2015.

[2] S. D. Blunt, M. R. Cook, and J. Stiles, "Embedding information into radar emissions via waveform implementation," in *2010 International Waveform Diversity and Design Conference*, Aug 2010, pp. 195–199.

[3] C. Sturm and W. Wiesbeck, "Waveform design and signal processing aspects for fusion of wireless communications and radar sensing," *Proceedings of the IEEE*, vol. 99, no. 7, pp. 1236–1259, July 2011.

[4] A. Hassanien, M. G. Amin, Y. D. Zhang, and F. Ahmad, "A dual function radar-communications system using sidelobe control and waveform diversity," in *2015 IEEE Radar Conference (RadarCon)*, May 2015, pp. 1260–1263.

[5] J. G. Metcalf, C. Sahin, S. D. Blunt, and M. Rangaswamy, "Analysis of symbol-design strategies for intrapulse radar-embedded communications," *IEEE Transactions on Aerospace and Electronic Systems*, vol. 51, no. 4, pp. 2914–2931, Oct 2015.

[6] A. de Oliveira, R. Sampaio-Neto, and J. M. Fortes, "Robust radar-embedded sidelobe level modulation using constrained optimization design," in *2016 IEEE Radar Conference (RadarConf)*, May 2016, pp. 1–5.

[7] B. Paul, A. R. Chiriyath, and D. W. Bliss, "Joint communications and radar performance bounds under continuous waveform optimization: The waveform awakens," in *2016 IEEE Radar Conference (RadarConf)*, May 2016, pp. 1–6.

[8] J. T. Reed, J. L. Odom, R. T. Causey, and A. D. Lanterman, "Gaussian multiple access channels for radar and communications spectrum sharing," in *2016 IEEE Radar Conference (RadarConf)*, May 2016, pp. 1–6.

[9] M. Scharrenbroich and M. Zatman, "Joint radar-communications resource management," in *2016 IEEE Radar Conference (RadarConf)*, May 2016, pp. 1–6.

[10] B. Li and A. Petropulu, "MIMO radar and communication spectrum sharing with clutter mitigation," in *2016 IEEE Radar Conference (RadarConf)*, May 2016, pp. 1–6.

[11] F. Hessar and S. Roy, "Spectrum sharing between a surveillance radar and secondary Wi-Fi networks," *IEEE Transactions on Aerospace and Electronic Systems*, vol. 52, no. 3, pp. 1434–1448, June 2016.

[12] C. Sahin, J. Jakabosky, P. M. McCormick, J. G. Metcalf, and S. D. Blunt, "A novel approach for embedding communication symbols into physical radar waveforms," in *2017 IEEE Radar Conference (RadarConf)*, May 2017, pp. 1498–1503.

[13] P. M. McCormick, S. D. Blunt, and J. G. Metcalf, "Simultaneous radar and communications emissions from a common aperture, Part I: Theory," in *2017 IEEE Radar Conference (RadarConf)*, May 2017, pp. 1685–1690.

[14] P. M. McCormick, B. Ravenscroft, S. D. Blunt, A. J. Duly, and J. G. Metcalf, "Simultaneous radar and communication emissions from a common aperture, Part II: Experimentation," in *2017 IEEE Radar Conference (RadarConf)*, May 2017, pp. 1697–1702.

[15] B. Ravenscroft, P. M. McCormick, S. D. Blunt, J. Jakabosky, and J. G. Metcalf, "Tandem-hopped OFDM communications in spectral gaps of FM noise radar," in *2017 IEEE Radar Conference (RadarConf)*, May 2017, pp. 1262–1267.

[16] S. Blunt and E. Perrins, *Radar & Communication Spectrum Sharing*. IET, 2018.

[17] J. Jakabosky, S. D. Blunt, and B. Himed, "Waveform design and receive processing for nonrecurrent nonlinear FMCW radar," in *2015 IEEE Radar Conference (RadarCon)*, May 2015, pp. 1376–1381.

[18] J. Jakabosky, S. Blunt, and B. Himed, "Spectral-shape optimized FM noise radar for pulse agility," in *2016 IEEE Radar Conference (RadarConf)*, May 2016, pp. 1–6.

[19] J. Jakabosky, B. Ravenscroft, S. D. Blunt, and A. Martone, "Gapped spectrum shaping for tandem-hopped radar/communications cognitive sensing," in *2016 IEEE Radar Conference (RadarConf)*, May 2016, pp. 1–6.

[20] B. Ravenscroft, S. Blunt, C. Allen, A. Martone, and K. Sherbondy, "Analysis of spectral notching in FM noise radar using measured interference," in *2017 IET International Radar Conference*, Oct 2017, pp. 1–6.

[21] A. Bahai, B. Saltzberg, and M. Ergen, *Multi-carrier digital communications: theory and applications of OFDM*. Springer, 2004.

[22] J. Jakabosky, L. Ryan, and S. Blunt, "Transmitter-in-the-loop optimization of distorted OFDM radar emissions," in *2013 IEEE Radar Conference (RadarCon13)*, April 2013, pp. 1–5.

[23] S. C. Thompson, A. U. Ahmed, J. G. Proakis, J. R. Zeidler, and M. J. Geile, "Constant envelope OFDM," *IEEE Transactions on Communications*, vol. 56, no. 8, pp. 1300–1312, August 2008.

[24] S. C. Thompson and J. P. Stralka, "Constant envelope OFDM for power-efficient radar and data communications," in *2009 International Waveform Diversity and Design Conference*, Feb 2009, pp. 291–295.

[25] M. P. Wylie-Green, E. Perrins, and T. Svensson, "Introduction to CPM-SC-FDMA: A novel multiple-access power-efficient transmission scheme," *IEEE Transactions on Communications*, vol. 59, no. 7, pp. 1904–1915, July 2011.

[26] S. D. Blunt, M. Cook, J. Jakabosky, J. D. Graaf, and E. Perrins, "Polyphase-coded FM (PCFM) radar waveforms, Part I: Implementation," *IEEE Transactions on Aerospace and Electronic Systems*, vol. 50, no. 3, pp. 2218–2229, July 2014.

[27] Y. Rahmatallah and S. Mohan, "Peak-to-average power ratio reduction in OFDM systems: A survey and taxonomy," *IEEE Communications Surveys Tutorials*, vol. 15, no. 4, pp. 1567–1592, FourthQuarter 2013.